An Investigation of the Impact Experimental Equipment Parameters Have on Synthetic Slag Behaviors in an Oxidative Environment Using a Confocal Laser Microscope

Carlos Ortiz, Jinichiro Nakano, Anna Nakano and James Bennett

Abstract In this research, experimental parameters of the confocal scanning laser microscope (CSLM) system were investigated to understand their impact on artifact changes in the melting and crystallization behaviors of synthetic slag in an oxidizing environment as it underwent rapid changes in gas flow, heating, and cooling rates. This study aims to provide CSLM users with fundamental information in utilizing CSLM equipment to investigate molten and solid slag behaviors.

Keywords Slag · Refractory · Gasification · Confocal scanning laser microscope (CSLM)

Introduction

High temperature environmental confocal scanning laser microscopy (CSLM) is an imaging technique that can provide high-resolution images and videos of phase changes under various conditions. CSLM has been used, for example, to study various in situ slag behaviors including crystallization and interaction with refractory materials under gasification conditions [1, 2]. In gasification, slag forms from mineral impurities in the carbon feedstock and flows down the refractory-lined sidewall of the gasification chamber [3]. The slag typically experiences rapid changes in temperature and oxygen partial pressure depending on location in a gasifier and its residence time. Crystallization and melting are influenced by slag chemistry, heating, and atmosphere, and are known to have a direct impact on gasification temperature and slag viscosity [4]. To study slag behaviors on a laboratory scale, rational interpretations of

---

C. Ortiz (✉) · J. Nakano · A. Nakano · J. Bennett
U.S. Department of Energy National Energy Technology Laboratory, 1450 Queen Ave., Albany, OR 97321, USA
e-mail: carlos.ortiz@netl.doe.gov

C. Ortiz
Oak Ridge Institute for Science and Education, Oak Ridge, USA

J. Nakano · A. Nakano
Leidos Research Support Team, Albany, USA

empirical readings are critical to understand outcomes but may become complicated because results would be affected by experimental parameter settings. This paper focuses on the use of CSLM to observe slag behavior in real time under variable experimental conditions in order to provide fundamental information that will help develop methodologies for future slag studies and minimize potential artifact in the measurements obtained.

Experimental Setup

Pre-melted synthetic slag's behaviors upon various heating, cooling, and gas flow rates were studied based on in situ observations using a high temperature environmental confocal scanning laser microscope (CSLM—Lasertec VL2000DX) with a heating chamber capable of heating samples above 2000 °C with appropriate thermocouples. A simplified schematic of the CSLM heating chamber used in this study is shown in Fig. 1.

Real-time high-resolution images of slag behavior were obtained using the CSLM system that used a violet diode laser with a wavelength of 406 nm. A synthetic slag similar to that found on a gasifier refractory surface by Bennett (2016) was prepared by mixing reagent grade oxide powders (Al_2O_3, CaO, Fe_2O_3, K_2O, MgO, and SiO_2) which were mixed and placed in a cylindrical platinum crucible (99.99% Pt; dimensions = 5 mm D × 5 mm OD by 0.4 mm wall thickness) [6]. The platinum crucible was then placed on a high-density alumina crucible (dimensions = 8 mm D × 5 mm OD by 0.5 mm wall thickness) and positioned inside the gold-plated CSLM furnace with an observation quartz window directly above the sample as shown in Fig. 1a. The chemical composition of the powder mixture was analyzed by an X-ray fluorescent technique (XRF—Rigaku ZSX Primus II) and is shown in Table 1. The mixture was then pre-melted by heating at 1873 K for 30 min in air to ensure full melting, then cooled to room temperature at 4300 K/min, cooling conditions that prevented crystallization. The resulting slag weighed approximately 0.1 g. In this setup, a platinum pan holding the Pt sample crucible inside the alumina crucible was located on one of the heating focal points and acted as the tip of a type R thermocouple (Fig. 1b). A halogen lamp used as the heat source and was located
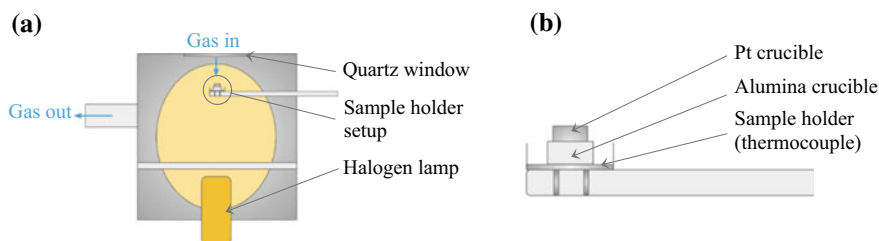

(a) Gas in / Quartz window / Sample holder setup / Halogen lamp / Gas out

(b) Pt crucible / Alumina crucible / Sample holder (thermocouple)

Fig. 1 A schematic of CSLM showing **a** the hot-stage and **b** the sample holder setup

Table 1 Chemical composition of power mixture prior to pre-melt

Oxide	Al_2O_3	CaO	Fe_2O_3	K_2O	MgO	SiO_2
Wt pct	0.8%	2.7%	34.6%	1.3%	0.9%	59.7%

at the other heating focal point. The temperature measured by the thermocouple of the sample holder commonly deviates from that at the sample inside the crucible depending on relative locations to the heating focal point (horizontally and vertically). Other parameters such as heating and gas flow rates also affect temperature readings. Prior to experiments, temperature deviation was estimated by calibration with high purity Pd (99.95%) beads of approximately 0.2 mg with a known melting temperature ($T_m = 1828$ K). Calibration was conducted under various heating and flow rates to investigate the effect of those on measurements of liquidus as a reference. The investigated heating rates were 400, 600, 900, and 1200 K/min while the studied flow rates were 0, 300, and 500 cm^3/min.

The effect of heating and gas flow rates on the slag behaviors was studied by heating the pre-melted slag to a target of 1873 K in a synthetic air environment (79% N_2, 21% O_2) at four different proportional–integral–derivative (PID) controlled heating rates and three different flow rates controlled by mass flow controllers (Alicat), for a total of 12 experimental runs. These experiments were conducted in the order from lowest to highest heating rate (100, 300, 600, 900 K/min). At each heating rate, three runs were performed with varying gas flow rates from highest to lowest (500, 250, 0 cm^3/min). During each run, the sample was held at 1873 K for 10 min and then cooled to room temperature at 4300 K/min. Upon heating, solid precipitates appeared around 1500–1650 K, which will be discussed in the results section. In order to discuss the effect of heating and flow rates on the temperature readings, the temperature at which the last observable surface precipitates in the slag sample completely melted, defined as T_1 in this study, was recorded for all experimental conditions. Slag behaviors were also studied during cooling to supplement observations made during the heating runs. For the cooling experiments, the sample was first heated to 1873 K, held for 10 min, and then cooled to room temperature at 100 K/min. The same sample was repeatedly used for all experiments. The spatial effect on temperature measurement was also investigated to determine its sensitivity and potential artifact on readings. The crucible with slag was placed at five different locations at the platinum pan and heated to 1873 K at a rate of 800 K/min with no gas flow during each run while the observed melting temperature of the surface precipitates (T_1) was recorded.

Results and Discussion

Effects on Temperature Calibration

The measured melting temperature of Pd versus the instantaneous heating rate and flow rate is shown in Fig. 2a, b. The instantaneous heating rate was obtained by taking a defined temperature range of data points around the temperature of interest, dividing them by the corresponding time range, and averaging the results. As seen in Fig. 2a, b the measured temperature for Pd melting was lower than that expected, indicating that the temperature inside the Pt crucible was appreciably higher than that at the bottom side of the sample holder, specifically at the point where the thermocouple reading takes place. As the heating rate increased, this difference became greater, indicating the sample area was heated faster than the thermocouple at faster heating rates. A delay in heating caused a relative deviation to appear in temperature readings. Contrarily, Fig. 2b shows that the measured temperature for Pd melting increases with gas flow rate. This relationship was expected because the gas flow was directed straight onto the sample area in the present experimental setup, directly cooling the sample.

The Effect of Crucible Position

Sample temperature is expected to be influenced by the distance (horizontally and vertically) from the heating focal point as mentioned in the experimental section. Five different sample locations on the sample holder pan were tested as shown in Fig. 3d. Figure 3a shows the effect of crucible position relative to the sample holder
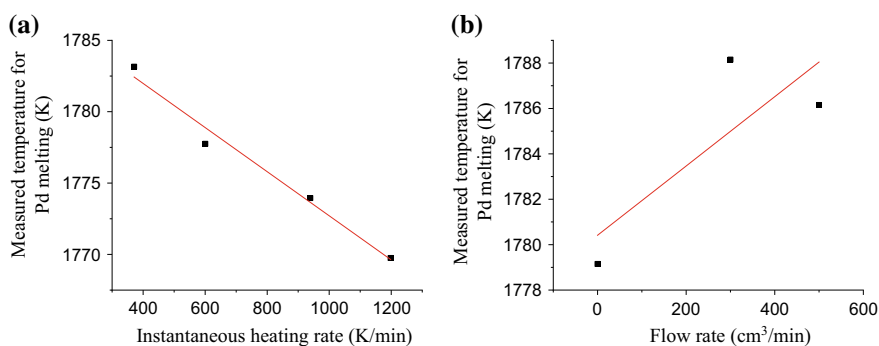

Fig. 2 Effect of experimental parameters on temperature calibration. **a** Measured temperature for Pd melting versus heating rate at flow rate = 0 cm^3/min. **b** measured temperature for Pd melting versus flow rate at heating rate = 20 K/min. Straight fitted lines are only for guiding with no significant implication
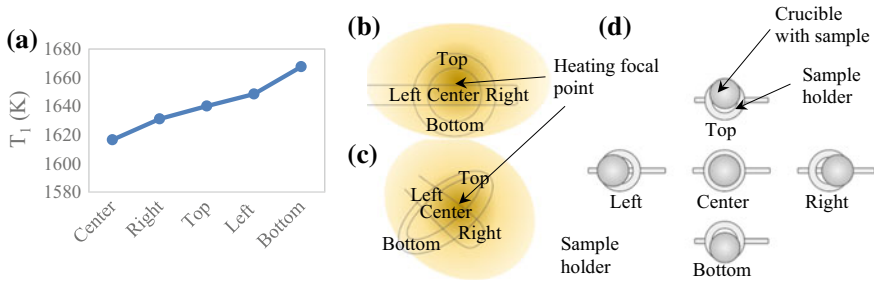
Fig. 3 Effect of crucible location relative to sample holder. **a** Measured temperature when last surface precipitate melts (T_1) at five different crucible locations. Heating rate = 800 K/min, flow rate = 0 cm³/min. **b** Schematic showing an offset of the irregularly shaped focal point. **c** Schematic showing a tilt of the sample holder. **d** Top view of crucible position at the platinum pan

on T_1, with the lowest temperature value measured when the crucible was located in the center of the sample holder.

This implies that at this location, a distance between the sample and the heating focal point was shortest. When the sample was moved away from the center, the distance from the focal point increased and the temperature experienced by the sample became lower than that measured at the thermocouple, resulting in a higher measured value for T_1. Figure 3a indicates that there might be a tilt of the platinum pan and that the focal point may not be a perfect sphere but rather irregular. These also indicate the heating focal point might be slightly off center. Figure 3b, c show an illustration of how the sample holder could be set up to produce the results given in Fig. 3a, with the tilt being exaggerated for demonstration purposes. About 40° temperature deviation was noted across the platinum pan, which implies spatial influences must be takin into account in temperature readings.

Melting and Crystallization of Slag

A representation of the crystallization and melting behaviors of the slag sample upon heating is shown in Fig. 4. Only a small portion of the slag, approximately 400 μm across, was visible due to the formation of a meniscus at the bottom of the crucible. For the sample shown in Fig. 4, a heating rate of 1000 K/min was used to heat the slag from room temperature to 1873 K and air was purged at a flow rate of 500 cm³/min. Figure 4(2) shows the formation of new structures on the surface of the slag around 1500 K, which will be referred to as precipitates hereafter. Upon approaching this temperature, part of the slag began to melt and enabled liquid-state diffusion, kinetically allowing solid precipitation, which had been thermodynamically stable at and below this temperature. As the temperature increased, more precipitates rapidly formed and the entire visible surface (Fig. 4(3)). The precipitates then began to melt around 1650–1700 K. A secondary liquid phase
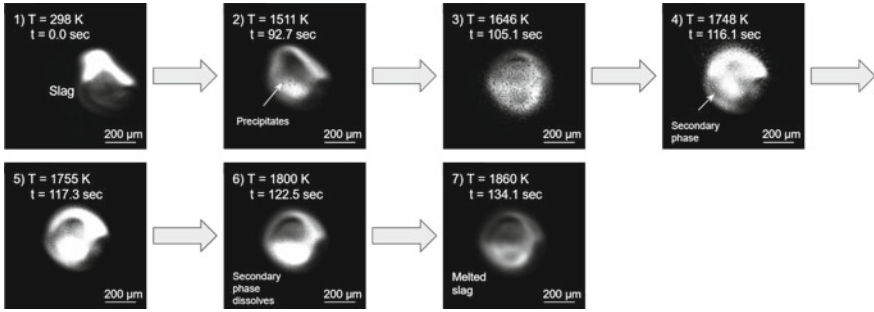
Fig. 4 CSLM successive images of the slag behavior upon heating in air. Heating rate = 1000 K/min. Flow rate = 500 cm^3/min. (1) Solid slag at room temperature (starting state). (2) Upon heating, first precipitates observed around 1500 K. (3) More precipitates formed and then began to melt. (4) A secondary liquid phase appeared (white droplets in images). (5) Surface precipitates completely melted while the secondary liquid remained (T$_1$). (6) Secondary liquid began to dissolve. (7) Secondary liquid completely dissolved

originating from the melting precipitates started to appear as white circular structures under CSLM as seen in Fig. 4(4). Figure 4(5) serves as a visual representation of the sample when temperature T_1 was reached at which the last observable surface precipitates completely melted. The secondary liquid phase structures coalesced with one another and they remained stable during a certain temperature range before they began to dissolve in the primary slag at 1800 K (Fig. 4(6)). By approximately 1860 K, the secondary liquid phase structures have completely dissolved (Fig. 4(7)). This temperature, seemingly a miscibility gap boundary for two immiscible slags, was also recorded for all experimental conditions referred to as T_2. Identifications of the phases are underway.
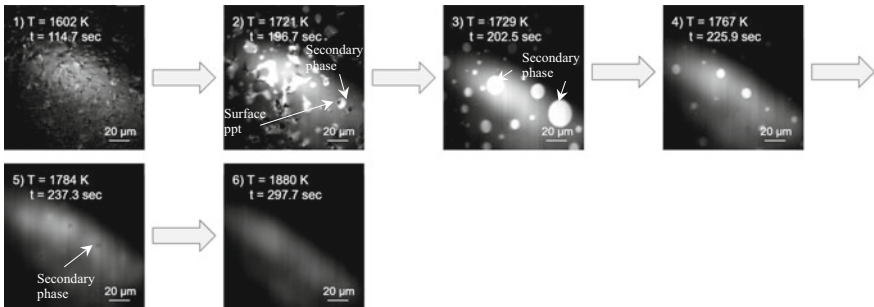

Fig. 5 CSLM high magnification images of the slag behavior upon heating in air. (1) Surface precipitates formed. (2) Surface precipitates melted and secondary liquid formed on the surface precipitates as they melted. (3) Secondary liquid remained after surface precipitates completely melted. (4) The secondary phase began to dissolve. (5) The secondary liquid almost completely dissolved. (6) The secondary liquid completely dissolved
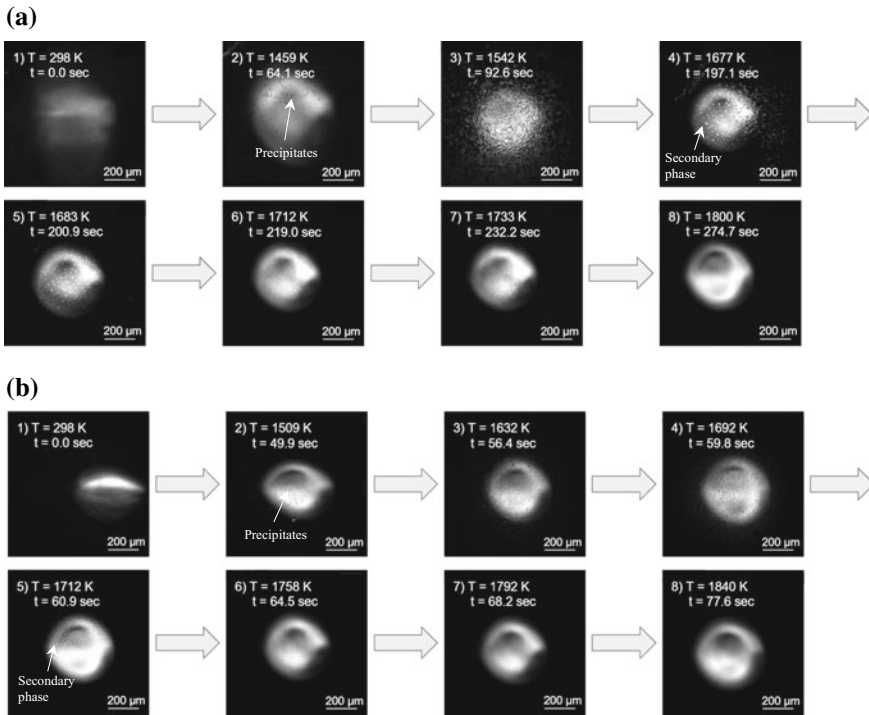
Fig. 6 Effect of heating rate on the slag behavior at an air flow rate of 250 cm^3/min. **a** Heating rate = 100 K/min. **b** Heating rate = 1500 K/min
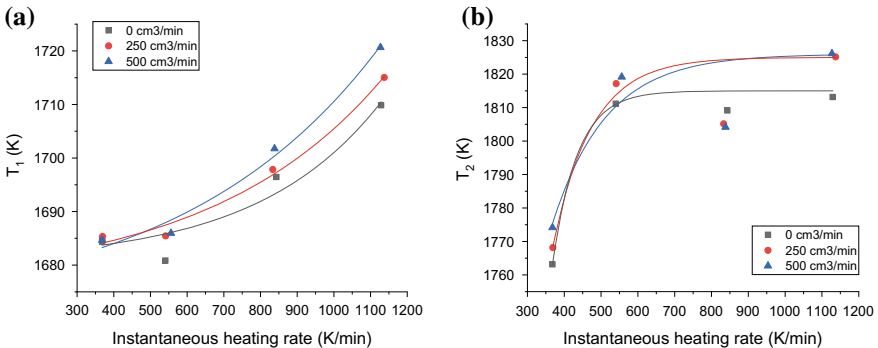

Fig. 7 Effect of heating rate and flow rate on melting behavior of slag and temperature readings. **a** measured temperature when last surface precipitate melts (T_1) versus instantaneous heating rate at different flow rates. **b** Measured temperature when secondary phase dissolves (T_2) versus instantaneous heating rate at different flow rates

To further investigate the phenomena, more images were taken at a higher magnification as shown in Fig. 5, which show the origination of the secondary liquid phase from the dark precipitates (Fig. 5(2)) and the dissolution of the secondary liquid phase (Fig. 5(5)). Figure 6a, b show the slag behaviors upon heating at the lowest heating rate (100 K/min) and highest heating rate (1500 K/min) used at a fixed air flow rate (250 cm^3/min). Both Fig. 6a, b show the successive events described in Fig. 4: the formation of the surface precipitates (second and third images), appearance of the secondary liquid phase (fourth image), melting of the surface precipitates (fifth image), and the dissolution of the secondary liquid phase (sixth image). As seen in Fig. 6, the size of the precipitates that first formed on the surface of the slag was significantly greater at the lower heating rate (third image in Fig. 6a, b). In both cases, the solid precipitation was thermally allowed through liquid-state diffusion while the low heating rate allowed more growth. The same was observed for the size of the secondary liquid phase, which was greater at the lower heating rate (fifth image in Fig. 6a, b). The higher heating rate minimized the formation and growth of the precipitates, likely because nucleation of the precipitates was impeded and growth was not sufficiently allowed in a shorter time in which the precipitates were temporarily going through the thermodynamically stable zone.

Figure 7a, b show the resulting T_1 and T_2, respectively, for various experimental conditions. A similar trend with flow rate variations observed in the temperature calibration (Fig. 2b) was also observed for T_1, where an increase in the measured temperature was noticed with an increasing flow rate. The same was observed for T_2 although the change seems less pronounced at higher flow rates (Fig. 7b). As mentioned in the temperature calibration section, this trend is caused by the cooling effect from the gas flowing directly onto the sample from the top, which allows the temperature measured at the thermocouple to "catch up" to that of the sample. On the other hand, both T_1 and T_2 increased with an increasing heating rate, which is the opposite of what was observed during the calibration runs. In contrast to the calibration runs, which were conducted with pure Pd beads, heating slag and reactions were influenced by other parameters such as heat conduction, convection, and incubation periods that affected the heat distribution to and within the slag sample. As a result, the temperature measured at the thermocouple below the sample level would be raised more rapidly. Still, the measured temperature at both events (T_1 and T_2) was affected by heating rate, which indicates that it is important to take this parameter into account when performing temperature readings by the present setup.

Since the same sample was repeatedly used for all experimental runs, the slag chemistry that may have changed due to volatilization over the course of the experiments and the deposition of evaporated material onto the chamber walls must be also considered in readings. Although a change in chemistry could contribute to changes in T_1 and T_2 with each run, it was found that only 0.98 wt% of the starting slag mass was lost after all of the experiments, indicating that the change in chemistry due to volatilization was minimal in this work. However, the small amount of material that vaporized may deposit on the gold-plated walls as heating progresses, which would interfere with the heating ability of the furnace since its design uses reflection from
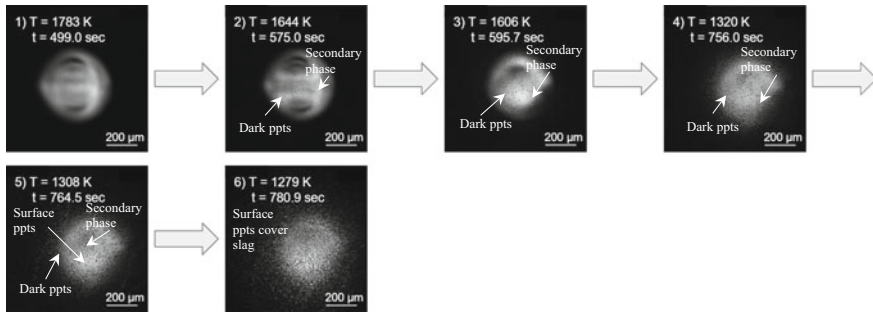
Fig. 8 CSLM images of the crystallization process of surface slag. Cooling rate = 100 K/min. Flow rate = 500 cm^3/min. (1) Melted single-phase slag. (2) Dark and white precipitates (secondary liquid phase) appeared during cooling. (3–4) Precipitates grew in size and number. (5) Dark precipitates formed on the surface, specifically on top of white droplets. (6) Dark precipitates covered the entire visible surface of the slag

the walls to direct heat to the sample area. Note in the present work, the furnace interior was continuously cleaned at each experiment. No evidence of iron diffusion was found on the alumina crucible side, indicating the interaction between iron oxide and the platinum crucible may have been minimal. This type of interaction is also not favored thermodynamically under an oxidizing environment; thus, it is very unlikely a change in chemistry could have impacted the results.

Figure 8 shows a representative crystallization behavior of the slag on cooling. For the sample shown here, a cooling rate of 100 K/min was used to cool the slag from 1873 K to room temperature at a gas flow rate (air) of 500 cm^3/min. At around 1300 K, dark precipitates surface began to form and cover the secondary phase (Fig. 8(5)). By approximately 1280 K, these precipitates covered the entire surface. The secondary liquid phase (white droplets in images), which was observed during the heating experiments at a temperature range around 1300–1770 K under the conditions used, was also noted on cooling around 1650–1830 K. Hysteresis between melting and formation temperatures may be due to delays caused by kinetics.

High magnification images during the slag crystallization process on cooling are shown in Figs. 9 and 10. These images show the formation of the secondary liquid phase on cooling with greater detail (Fig. 9(2)). The secondary liquid droplets also grew by coalescing with one another until diffusion was impeded at a low temperature and increased viscosity (Fig. 9(5)). Figure 10 shows coalescing of two secondary phase droplets. Dark particles began to form in between the secondary liquid (Fig. 9(3)). Figure 9(6) shows the dark surface precipitates that formed around 1300 K, which seemed to cover only the secondary phase and not the dark precipitates in between. It is possible that the surface precipitates grew from the secondary liquid phase and that such transformation was not fully completed because cooling further proceeded where the thermodynamic stability of the phase or formation kinetics was affected by the lower temperatures. Identifications of the phases are underway.
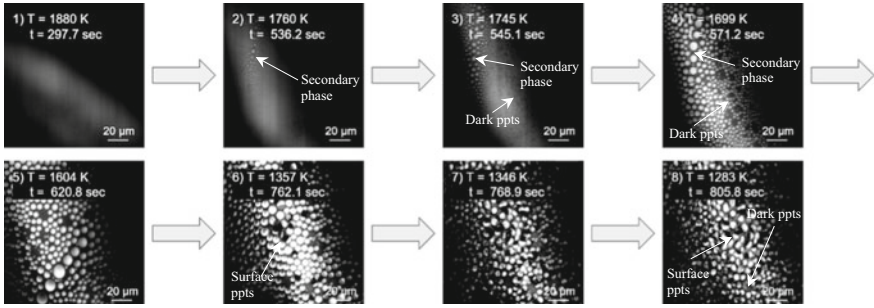
Fig. 9 CSLM high magnification images of crystallization process of surface slag during cooling. Cooling rate = 100 K/min. Flow rate = 0 cm^3/min. (1) Melted slag with some secondary liquid phase droplets formed. (2) Secondary liquid phase droplets grew. (3) Dark precipitates appeared as droplets grew. (4) White and dark precipitates grew. (5) Precipitates stopped moving and growing. (6) Dark precipitates began covering surface. (7–8) Dark surface precipitates covered entire field of view, mainly the white droplets
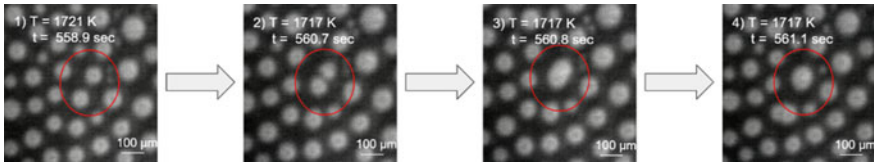
Fig. 10 CSLM images showing the moment of coalescing of the secondary liquid phase on cooling. Cooling rate = 100 K/min. Flow rate = 0 cm^3/min

Conclusion

The CSLM was used to study the crystallization and melting behaviors of synthetic slag in an oxidizing atmosphere under different controlled experimental conditions. The formation of a secondary liquid phase was observed during both heating and cooling, and its liquidus temperatures were compared to understand slag behaviors under varying conditions. The measured temperatures for the melting of Pd and for precipitate formation and dissolution of the secondary phase were affected by the choice of heating rate and flow rate. Crucible position on the sample holder and sample holder tilt impacted the distance between the sample and the heating focal point and caused a significant variance in the results. The present results suggest these are important parameters to consider when performing temperature readings using a CSLM system.

References

1. Nakano J, Sridhar S, Moss T, Bennett J (2009) Crystallization of synthetic coal-petcoke slag mixtures simulating those encountered in entrained bed slagging gasifiers. Energy Fuels 23:4723–4733
2. Nakano J, Sridhar S, Moss T, Bennett J, Kwong K (2001) Interactions of refractory materials with molten gasifier slags. Int J Hydrogen Energy 36:4595–4604
3. Kwong K, Petty A, Bennett J, Krabbe R, Thomas H (2007) Wear mechanisms of chromia refractories in slagging gasifiers. Appl Ceram Technol 4(6):503–513
4. Cormos CC, Starr F, Tzimas E (2010) Use of lower grade coals in IGCC plants with carbon capture for the co-production of hydrogen and electricity. Int J Hydrogen Energy 35:556–567
5. Yin H, Emi T, Shibata H (1999) Morphological instability of δ-ferrite/γ-austenite interphase boundary in low carbon steels. Acta Mater 47:1523–1535
6. Bennett J, Nakano J, Nakano A, Thomas H (2016) Gasification slag and the mechanisms by which phosphorous additions reduce slag wear and corrosion in high Cr_2O_3 refractories